JOURNAL DE PHYSIQUE
Colloque C1, supplément au n°10, Tome 43, octobre 1982

SEM CHARACTERIZATION OF EFG POLYCRYSTALLINE SILICON SOLAR CELLS REALIZED BY ION IMPLANTATION AND LASER ANNEALING WITH OVERLAPPING PULSES

J.C. Muller, P. Siffert, C.T. Ho*, J.I. Hanoka* and F.V. Wald*

Centre de Recherches Nucléaires, Laboratoire de Physique et Applications des Semiconducteurs (PHASE), 67037 Strasbourg Cedex, France

**Mobil Tyco Solar Energy Corporation, 16 Hickory Drive, Waltham, Massachusetts 02254, U.S.A.*

Résumé. On a étudié par microscopie électronique (SEM) et par EBIC des cellules solaires préparées sur du silicium polycristallin en ruban de type EFG dont la jonction était réalisée par incrustation (AMI) d'ions atomiques et moléculaires issus d'une source contenant PF_5. La recristallisation du dommage était effectuée par recuit laser pulsé Nd-YAG.

Alors qu'au voisinage de la surface la recombinaison des porteurs est due essentiellement aux recouvrements des impulsions laser (diamètre 100 µm, taux de répétition 10 kHz), on constate qu'aux profondeurs plus grandes la recombinaison aux joints de grains est dominante. La recristallisation par épitaxie en phase liquide conserve exactement la structure polycristalline sous-jacente.

Abstract. Atomic and molecular ion implantation (AMI) of non mass separated PF_5 ions has been used to form the N^+ layer on EFG ribbon. A pulsed Nd-YAG laser operating at a high repetition rate (10 kHz) was then employed to anneal the amorphized layer via liquid phase epitaxy.

The properties of the recrystallized layers have been analyzed by SEM with secondary electron micrography and EBIC. The following results have been observed. At low electron beam energies (below 12 keV), strong EBIC recombination currents resulting from the overlapping laser pulses is clearly visible. At higher energies (above 20 keV), the recombination due to the grain boundaries in the ribbon becomes dominant. The regrowth after annealing replicates exactly the underlying structure. Finally, some electrical characteristics of the doped layers (doping profile) as well as the photovoltaïc performance are presented. Efficiencies up to 11 % have been obtained under AM1 conditions.

1. Introduction

Ion implantation, followed by a pulsed annealing treatment in the liquide phase regime induced by either laser or electron beams, is now considered to fulfill the requirements of low-cost silicon solar cell mass production. As substrate materials, both cast polycristalline bulk and ribbon silicon, especially EFG ribbon, constitute the most promising candidates. Therefore, it is important to demonstrate how these large grain sheets, which contain a variety of defects and inhomogeneities, both in the bulk and at the surface, react to the doping performed with the atomic and molecular ion implantation (AMI) procedure, followed by a high repetition rate (10 kHz) pulsed Nd-YAG laser annealing.

The goal of this study was to investigate by SEM and EBIC the behavior of the doped layer after individual laser pulses (100 µm in diameter) have melted the surface. Furthermore, this technique gives information on the surface recombination in the annealed zone, as well as on the quality of regrowth of each grain. For example, an EBIC line scan gives a relative measure of charge collection between

two adjacent grains. A characteristic property of such polycristalline silicon can be a nonuniform penetration of the dopants during implantation due to channeling conditions, which change with the orientation of each individual grain. The doping profile has been measured by anodic stripping as well as by SIMS. Finally, the photovoltaïc performance of these cells is considered.

2. Experimental conditions

A. EFG Samples

The ribbon samples were selected from material grown in closed shape form (1). Some of the samples have been heat treated at 900°C under PH_3 ambient for 30 minutes followed by a slow cool down to 650°C to improve the minority carrier lifetime.

B. Junction Formation

An unanalyzed beam of molecular and atomic ions was extracted from the ion source filled with PF_5 and accelerated to 10 keV before impinging directly into the sample (2). The implanted ion dose was up to 10^{17} cm^2.

Regrowth of the fully amorphized layer was obtained by using a Nd-YAG laser "Epitherm"-system (3), emitting at 5300 Å. The repetition rate of the pulses of this system can be as high as 10 kHz, the pulse duration being 100 nanoseconds and the beam diameter 0.1 mm after focusing. In the single mode regime, the energy densities up to 3 J/cm^2 can be obtained. Large areas are covered by a microprocessor controlled setup, which allows predetermined pulse overlaps.

C. SEM Measurements

A Cambridge S4-10 SEM which was operated at various beam energies from $\simeq$ 5 keV to 30 keV was used so that both surface and bulk effects could be distinguished. A Keithley 427 current amplifier was employed to amplify the EBIC signal and feed it back to the SEM video display (4). Grain orientation was determined using the selected area diffraction mode of the SEM.

D. Solar Cell Processing

After the junction was created, cell fabrication was completed with screen printed and alloyed aluminium contacts for the back surface field (BSF) and vacuum evaporation of Cr-Ti-Ag for the front contact grid. The metal contact was sintered at 450°C for 15 minutes in N_2, this heat treatment constituting also the post-laser thermal treatment (5). Finally, the cell front surface was covered by an antireflecting Si_3N_4 film.

3. Surface analysis

Figure 1(a) and (b) represent EBIC pictures of a periodically pulsed pattern for 10 keV and 30 keV electron energy. Some well-defined craters are visible, which are even enhanced on the secondary image of the same zone (figure 1(c)). The usual pulsed pattern has little effect on the surface topography, except when craters appear. At low energies (figure 1 (a)) the periodic pattern dominates the recombination ; at higher energies (figure 1(b)) grain boundaries play the most important role. Il should be noted that within the craters center, electrical recombination activities can be seen clearly.

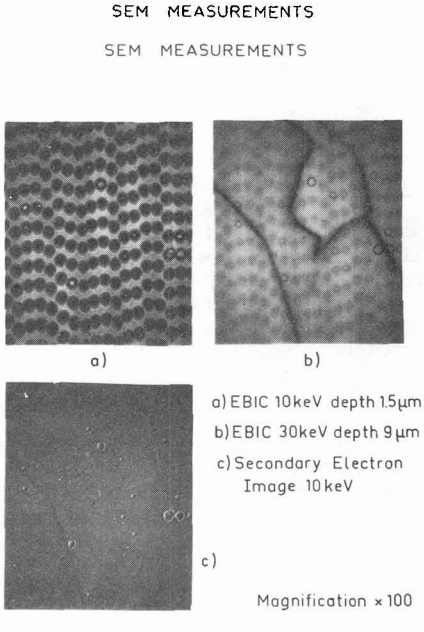

Fig. 1 : EBIC and secondary electron image of the grain boundary structure and pulse pattern for implanted EFG ribbon sheets annealed with a high repetition rate Nd-YAG laser.

Further details of the pulse annealed regions, the craters, and especially the effect of a grain boundary are shown in figure 2. It appears that when a grain boundary is intersected by a laser spot, the resulting molten area is no longer circular but has a lenticular shape along the grain boundary direction (clearly visible on the secondary image of figure 2 (a). Also, it appears that the EBIC image shows a lip-like structure with somewhat less recombination along the line of the grain boundary. Finally, note that the centers of the craters show a high degree of recombination.

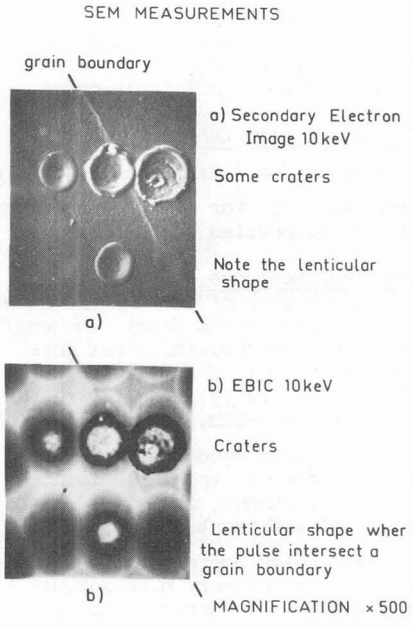

Fig. 2 : EBIC and secondary electron image given the detail of the pulsed pattern for the same sheet.

4. Solar Cell Evaluation

A. Dark I-V Characteristics

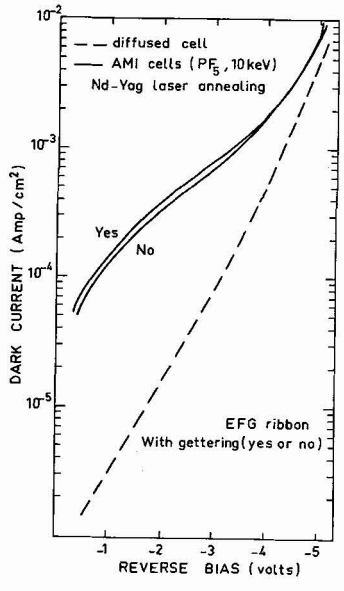

Fig. 3 : Reverse dark current of AMI cells together with a classical diffused cell.

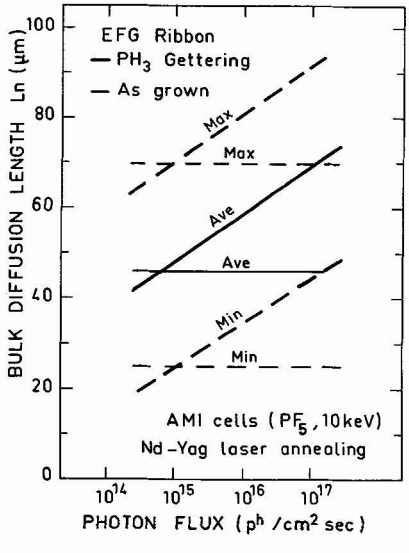

Fig. 4 : Evolution of the bulk diffusion length L_n for PH_3 treated cells as compared to "as grown" cells.

As shown in Figure 3, the junction space charge recombination current densities for the ion beam and laser annealed cells are more than one order of magnitude higher than for a standard diffused cell. However, it should be mentioned that no chemical handling is necessary for junction manufacturing with ion beams.

B. Bulk Diffusion Length L_n

Just as for diffused cells, the diffusion length L_n in EFG cells varies with illumination (6) for AMI processed structures (figure 4). Gettering treatments improve the properties of the material, as is the case for diffused cells.

C. Spectral Response

The response of the AMI and laser processed cell on the short wavelength side of the spectrum falls off more rapidly than that of a diffused control cell (figure 5). This may result from several effects, especially from:

- A high surface recombination velocity due either to the implantation, the laser treatment, or to the absence of chemical treatments.

- The very high doping of the surface layer, due to the very high solubility of the active phosphorus, which increases the light absorption in the short wavelength end of the spectrum.

- The deep junction, due to laser melting (see below).

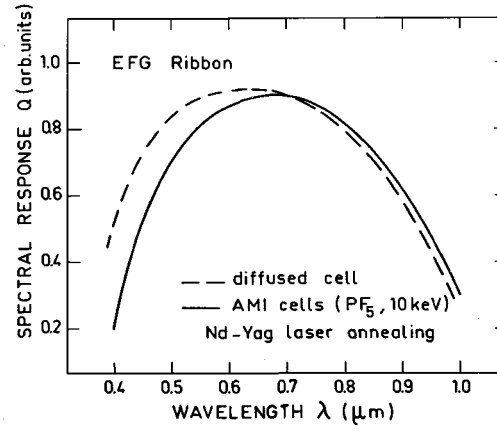

Fig. 5 : Spectral response of a AMI cell and a classical diffused test cell.

D. Phosphorus Dopant Profile

Both SIMS and anodic stripping have shown that the distribution of phosphorus is nearly exponential, leading to a junction depth as deep as 1 μm, both in EFG and in single-crystal samples. Even if the implanted dopants are less than 1000 Å from the surface after the AMI process, they are fully redistributed after laser treatment.

E. Cell Performance

The AM1 efficiencies of the AMI processed large scale (>10 cm^2) cells are reported in Table I. After gettering, efficiencies in excess of 11 % have been obtained.

TABLE I

AM 1 EFFICIENCIES OF E.F.G. POLYCRISTALLINE SILICON CELLS OF 11 cm^2 AREA

Junction manufacturing	Laser annealing	Dark current (-1 v) (mA/cm^2)	V_{oc} (mV)	I_{sc} (mA/cm^2)	FF	η (%)
AMI 10 keV dosis: 10^{17} cm^{-2}	pulsed Yag system "Epitherm" 2.5 J/cm^2	0.56	531	28.1	0.66	9.9
		0.27	525	27.7	0.65	9.4
	thermal anneal by sintering of 450 °C 15 min.	0.67 §	554	29.5	0.68	11.2
		0.44 §	545	28.2	0.66	10.2

§ : these sheets have been gettered at 900 ° C for 30 min. in PH_3

5. EBIC Results and Discussion

Several interesting EBIC results appear from this investigation of laser processed polycystalline silicon :

- The grain boundary structure after melting replicates exaclty the underlying grain structure.

- Recombination has disappeared from the grain boundaries from the surface down to about 2 μm, the depth of phosphorus penetration. This constitutes an intriguing result as it indicates that molecular ion implantation associated with pulse annealing eliminates grain boundary recombination. There are at least two possible explanations for this effect : if impurities are responsible for the recombination at grain boundaries, they have been fully redistributed after the short time duration melting. Probably they are now concentrated in the dark circular areas associated with the periodic pulse patterns shown in the EBIC figures 1 and 7. Another possibilities is that there is a beneficial effect of fluorine on grain boundary dangling bonds or recombination centers, as it has been suggested to act in the same way as hydrogen.

The evidence supporting the contention of this recombination disappearance comes from the EBIC micrographs such as exemplified by figures 1(a) and 1(b). In ordinary polycrystalline silicon (i.e., not processed by AMI and recrystallized), grain boundary recombination manifests itself as shown in figure 1(b), that is as lines of dark contrast following the trace of the boundary. In figure 1(a), where the beam penetration was $\lesssim 2\,\mu$m, no such lines of dark contrast are seen.

- Differences in grain orientation can have a non-negligible effect if the implantation range is due to channeling : In figure 6 we see that at the edge of two grains A and B, having respectively the orientation <110> and <124>, the grain A has a significantly lower current collection than grain B. Figure 7 shows the diffraction photographs of A, B and the interface. This phenomena can be explained in terms of a more pronounced channeling effect in the <110> direction.

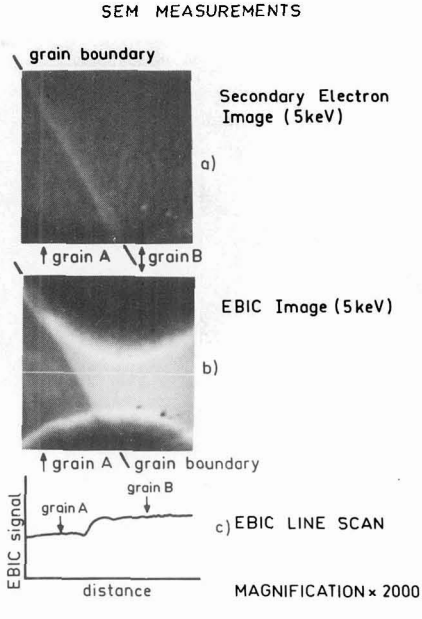

Fig. 6 : Difference in current collection between two adjacent grains seen by EBIC line scan.

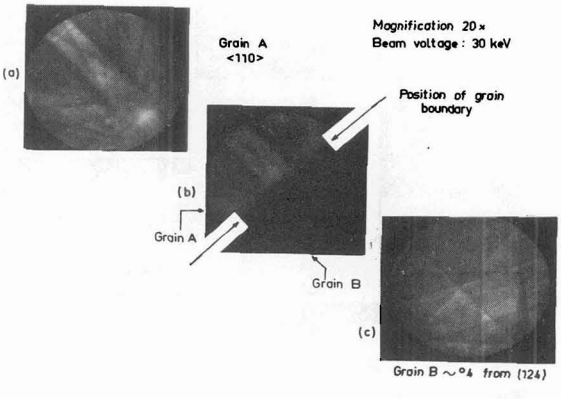

Fig. 7 : Selected area diffraction on the SEM given the orientation of the two observed grains.

6. Conclusion

The sharp diffraction images obtained after laser processing of the AMI implanted surfaces indicate that the crystallinity of the regrown material is quite good ; therefore, the presence of multiple regrown zones, corresponding to the laser used, has not affected the material's quality, as no amorphous residual zones are seen. However, recombination seems to be high near the center of the annealing spot where the power density of the Gaussian energy distribution is highest. Substantial microscopic defects still exist after the laser processing, as indicated both by dark and illuminated performance. However, cell performance in excess of 10 % are still possible, even over large areas (> 10 cm^2).

7. References

1. A.S. TAYLOR, R. STORMONT, C.C. CHAO and E.J. HENDERSON, 15th IEEE Photovoltaïc Specialists Conference Record (New York : IEEE : 1981), p. 589.

2. J.C. MULLER and P. SIFFERT, Inter.Workshop on Ion Implantation, Laser Treatment and Ion Beam Analysis of Materials. Bombay (India), Fev. 9-13 (1981), to be published in Radiation Effects (1982).

3. QUANTRONIX Smithtown N.Y. (USA).

4. J.I. HANOKA and R.O. BELL, Ann. Rev. Mat. Sci., Vol. 11 (Palo Alto, CA : Annual Reviews, Inc., 1981), p. 353.

5. F. ZIGNANI, R. GALLONI, L. PEDULLI, G.G. BENTINI, M. SERVIDORI, F. CEMBALI and A. DESALVO, 2th European Photovoltaïc Solar Energy Conf. Berlin (W.Germany) (1979) p. 213 Ed. D. REIDEL.

6. C.T. HO, R.O. BELL, F.V. WALD, Appl. Phys. Lett. 31 (1977) 463.